



Bowing the Wolf: Simulations and Experiments on a Real Cello

O. Inácio^a, J. Antunes^b and M.C.M. Wright^c

^a *Musical Acoustics Laboratory, ESMAE, Polytechnic Institute of Porto, Rua da Alegria 503, 4000-045 Porto, Portugal, octavioinacio@esmae-ipp.pt*

^b *Applied Dynamics Laboratory, Institute of Nuclear Technology, , 2686-953 Sacavém, Portugal, jantunes@itn.mces.pt*

^c *Institute of Sound and Vibration Research, University Road, Highfield Southampton S017 1BJ, UK, mcmw@isvr.soton.ac.uk*

ABSTRACT: Most theoretical papers on bowed-string instruments deal with isolated strings, pinned on fixed supports. In addition, the instrument body dynamics have been accounted using extremely simplified models of the string/body interaction through the instrument bridge. Such models have, nevertheless, been instrumental to the understanding of a very common and musically undesirable phenomenon known as the “wolf note” – a strong beating interplay between string and body vibrations. Cellos, bad and good, are particularly prone to this problem. In recent work our computational modal method has been extended to incorporate the complex dynamics of real-life instrument bodies, and their coupling to the string motions, using basic experimental dynamical body data. The string is modelled using its unconstrained modes, assuming pinned-pinned boundary conditions at the tailpiece and the nut. At the intermediary bridge location, the string/body coupling is enforced using the body impulse-response or modal data, as measured at the instrument bridge. In the present paper our computational approach is applied to a specific cello, which provided experimental wolf-behaviour data under several bowing conditions, as well as laboratory measurements of the bridge impulse responses on which the numerical simulations were based. Interesting aspects of the string/body dynamical responses are highlighted by our numerical simulations and the corresponding sounds and animations produced.

1. INTRODUCTION

In previous work we developed a modal method to deal with plucked and bowed strings [1-4], enabling an effective simulation of such systems, even when dispersive effects are significant. As in most other published work, our simulations assume a string pinned at the bridge and the nut, and therefore decoupled from the instrument body. Such approach proved adequate to obtain the typical motion patterns displayed by bowed-strings. However, because the bridge is assumed motionless, computations are obviously unable to cope with more subtle phenomena related to the coupling of string and body motions.

More recently our computational method was extended to incorporate the multi-modal dynamics of a cello body, fully coupled to the string motions [5]. It is a hybrid approach, in the sense that a theoretical model of the string is coupled with dynamical body data, stemming from either simplified models or real-life experiments.

The string is modelled using its unconstrained modes and, in contrast with our previous publications [1-4], assuming now pinned-pinned boundary conditions at the tailpiece and the nut. Then, at the bridge location, the string/body coupling is enforced using the body impulse-response or modal data (as measured at the bridge). At each time step, the system motion is computed by integrating the string modal equations, excited by the modal-projected values of

the frictional bow force and also of the string/bridge contact force. The latter is obtained from the body motion at each time-step, as computed either (a) using the body impulse-response, or (b) from a modal model of the body. In the first method, the body dynamics are obtained through incremental convolution, a costly procedure which however enables the direct simulation of real bodies without any further modelling assumptions or simplifications. The second method allows for faster computations, but demands a computed or identified modal model of the instrument body. After a few demonstrative experiments and a detailed presentation, our computational approaches are illustrated for typical self-excited string motion regimes of a cello. In particular, simulations pertaining to the so-called “wolf notes” are presented.

2. EXPERIMENTS

In order to illustrate the coupling between the body of the instrument and the strings, some preliminary experiments were carried on a cello. Mobility frequency response functions were measured at the bridge in the horizontal direction, through impact excitation, with the bridge response being sensed by an accelerometer. The highest amplitude body resonance occurs at approximately 196 Hz with a relatively low damping ratio (= 0.7%) when compared with the majority of higher frequency modes which reveal damping ratios of the order of 2%. This high amplitude mobility peak is responsible for a particular effect to which these instruments (bad or good) are known to be very susceptible: the wolf note. It is an unpopular phenomenon among musicians since it gives origin to harsh and beating-like sounds turning proper musical execution extremely difficult at some positions along the fingerboard. Although unpleasant for the listener, the emergence of this effect is paradigmatic of the importance of the body/string interaction.

Figure 1 depicts the typical amplitude-modulated waveform that characterizes the wolf note. In order to achieve this sound, the musician stopped the C_2 string at a distance approximately $L/3$ from the bridge (where L is the length of the string), for this instrument, playing the G_3 note at roughly 196 Hz. Clearly, the beating phenomena displayed is the result of strong coupling between the string vibration and the main body resonance, which is related to the proximity of their frequencies. Shortening the effective length of the string by a small amount is enough to prevent the wolf note to develop.

The wolf phenomenon has been the subject of several papers [6-10] the most generally accepted explanation being the one suggested by Schelleng [11], forty years ago. More recently the basis of this explanation has been revisited and further discussed by Woodhouse [12]. However, there are still a few aspects deserving exploration, such as the influence of the string dynamics in the portion between the tailpiece and the bridge.

On the other hand, we experienced a dependence of the wolf beating frequency on the bowing parameters, an aspect which seems absent from the literature. Also, the emergence of wolf phenomena appears to depend somewhat on the time-history of the bowing parameters. These issues will be addressed in the present and future papers.

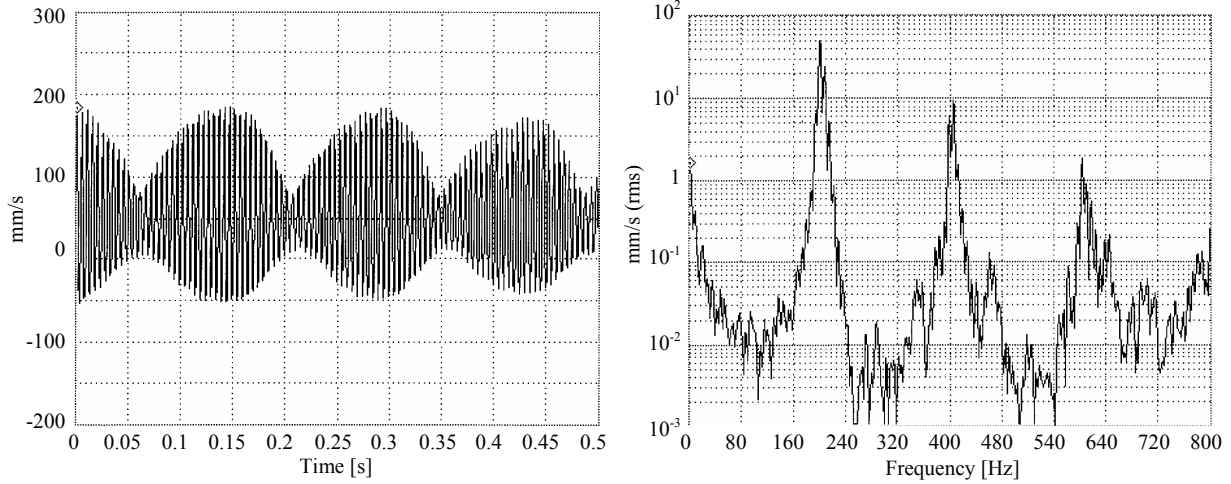


Figure 1 – Velocity time-history and spectrum of the bridge vibration, resulting from bowing on the C_2 string at a fingerboard position approximately $L/3$ from the bridge (generating here a wolf note).

3. COMPUTATIONAL METHOD

3.1 Formulation of the String Dynamics

Consider an ideal string of length L , linear density m and dissipation coefficient η , subject to a constant axial tensile force T and a force distribution $F(x,t)$. The small-amplitude transverse motion $y_s(x,t)$ of the string is described by the classic damped wave-equation:

$$m \frac{\partial^2 y_s}{\partial t^2} = T \frac{\partial^2 y_s}{\partial x^2} - \eta \frac{\partial y_s}{\partial t} + F(x,t) \quad (1)$$

where the wave speed is given by $c^2 = T/m$. Any solution of equation (1) can be formulated in terms of the string's modal parameters: for modeshapes normalised at unitary maximum values modal masses are given as $m_n = m \cdot L/2$ ($\forall n$). Other modal parameters are the circular frequencies $\omega_n = n\pi c/L$, damping values ζ_n and mode shapes $\varphi_n(x) = \sin(n\pi x/L)$, with $n = 1, 2, \dots, N$. The order N of modal truncation is problem-dependent and must be asserted by physical reasoning. On the modal space the forced response of the damped string is formulated as:

$$[M]\{\ddot{Q}(t)\} + [C]\{\dot{Q}(t)\} + [K]\{Q(t)\} = \{\Xi(t)\} \quad (2)$$

Where $[M] = \text{Diag}(m_1, \dots, m_N)$, $[C] = \text{Diag}(2m_1\omega_1\zeta_1, \dots, 2m_N\omega_N\zeta_N)$, $[K] = \text{Diag}(m_1\omega_1^2, \dots, m_N\omega_N^2)$, are the matrices of modal parameters, $\{Q(t)\} = \langle q_1(t), \dots, q_N(t) \rangle^T$ and $\{\Xi(t)\} = \langle \mathfrak{I}_1(t), \dots, \mathfrak{I}_N(t) \rangle^T$ are the vectors of modal responses and generalised forces, respectively. The damping values ζ_n are usually identified from experiments, however, they may eventually be theoretically

estimated. The modal forces $\mathfrak{F}_n(t)$ are obtained by projecting the external force field on the modal basis:

$$\mathfrak{F}_n(t) = \int_0^L F(x,t) \varphi_n(x) dx, (n=1,2,\dots,N) \quad (3)$$

The physical motions at any point of the string can be computed from the modal amplitudes $q_n(t)$ by superposition:

$$y(x,t) = \sum_{n=1}^N \varphi_n(x) q_n(t) \quad (4)$$

and similarly concerning the velocities and accelerations. For given external excitation and initial conditions, the previous system of equations can be integrated using an adequate time-step integration algorithm. Explicit integration methods are well suited for the friction model used here. In our implementation, we used a simple Velocity-Verlet integration algorithm, which is a low-order explicit scheme. Note that, although (2-4) obviously pertain to a linear formulation, nothing prevents us from including in $\mathfrak{F}_n(t)$ all nonlinear effects arising in the system. Accordingly, the system modes become coupled by the nonlinear effects.

For the present case, the external force field $F(x,t)$ is due to the excitation friction force $F_{s,a}(x_c,t)$ provided by the bow (which we will model in this paper as a single hair bow, although we can easily introduce excitation by a bow of finite width – see [4]), by the interaction force $F_b(x_b,t)$ between the body and the string at the bridge and by the possible presence of a finger on the fingerboard.

3.1.1 Friction Model

The friction force arising between the string and the bow hair at location x_c of the string is given by:

$$\begin{cases} F_s(x_c,t) = -\mu_d(\dot{y}_c) \frac{F_N}{b} \text{sgn}(\dot{y}_c); & \text{if } |\dot{y}_c| > 0 \\ |F_a(x_c,t)| < \mu_s \frac{F_N}{b}; & \text{if } |\dot{y}_c| = 0 \end{cases} \quad (5)$$

where F_N is the normal force between the bow and the string, μ_s is a “static” friction coefficient (used during surface adherence) and $\mu_d(\dot{y}_c)$ is a “dynamic” friction coefficient (used for sliding regimes). Here, the relative transverse velocity between the bow and the string is given by:

$$\dot{y}_c(t) = \dot{y}(x_c,t) - \dot{y}_{bow}(t) = \sum_{n=1}^N \varphi_n(x_c) \dot{q}_n(t) - \dot{y}_{bow}(t) \quad (6)$$

Recent research on friction models for bowed instruments [13] suggests the relevance of dynamical thermal phenomena in the tribology of rosin, which may induce hysteretic effects in the friction-velocity dependence. In spite of the unquestionable interest of such findings, we will use here the classical approach for sliding behaviour, as the present paper addresses a



different issue. We assume that $\mu_d(\dot{y}_c)$ is a function of the relative bow/string velocity, and use the following model:

$$\mu_d(\dot{y}_c) = \mu_D + (\mu_S - \mu_D) e^{-C|\dot{y}_c|} \quad (7)$$

where, $0 \leq \mu_D \leq \mu_S$ is an asymptotic lower limit of the friction coefficient when $|\dot{y}_c| \rightarrow \infty$, and parameter C controls the decay rate of the friction coefficient with the relative bow/string sliding velocity. The friction model (7) can be readily fitted to typical experimental data, by adjusting the empirical constants μ_S , μ_D and C .

The sliding behaviour, described by the first equation (5), does not cause problems for simulations, as this equation explicitly shows how the sliding force should be computed as a function of the sliding velocity. However, during adherence, simulation becomes more difficult. Indeed, the second equation (5) merely states a limiting value for the friction force, during adherence, and gives no hint on how $F_a(\dot{y}_c, t)$ may be actually computed. This is because the adherence force depends on the overall balance of all internal and external forces acting upon the system, which are quite complex for multi-degree of freedom problems. Most friction algorithms deal with this problem through implicit numerical schemes, which can be quite expensive to run. In our approach, an explicit procedure is used at each time-step, as explained in [1].

3.2 Formulation of the Body Dynamics

As previously explained, our method was implemented to simulate the influence of the string/body coupling using two different procedures: incremental convolution of a measured impulse response or through a modal model of the body dynamics.

3.2.1 Incremental Convolution Formulation

At the bridge, the string motion forces the cello body into vibration. The response of the body can be computed, at each time step i , by the incremental convolution of the time-history of the interaction force between the bridge and the string $F_b(x_b, t)$ and the body impulse response function at the same point x_b , according to equations (10) and (11).

$$y_b(x_b, t) = \int_0^t F_b(x_b, \tau) \cdot h(t - \tau) d\tau \quad ; \quad \dot{y}_b(x_b, t) = \int_0^t F_b(x_b, \tau) \cdot \dot{h}(t - \tau) d\tau \quad (10,11)$$

where $y_b(x_b, t)$ and $\dot{y}_b(x_b, t)$ are the displacement and velocity of the bridge at the contact point with the string, while $h(t)$ and $\dot{h}(t)$ are the displacement/force and velocity/force impulse response functions of the instrument body, measured at the bridge.

3.2.1 Modal Formulation

The response of the body of the instrument can be represented by a simplified modal model:

$$[M_B] \{\ddot{Q}_B(t)\} + [C_B] \{\dot{Q}_B(t)\} + [K_B] \{Q_B(t)\} = \{\Xi_B(t)\} \quad (12)$$

where $[M_B] = \text{Diag}(m_1^B, \dots, m_p^B)$, $[C_B] = \text{Diag}(2m_1^B \omega_1^B \zeta_1^B, \dots, 2m_p^B \omega_p^B \zeta_p^B)$, $[K_B] = \text{Diag}(m_1^B (\omega_1^B)^2, \dots, m_p^B (\omega_p^B)^2)$, are the matrices of the body modal parameters, $\{Q_B(t)\} = \langle q_1^B(t), \dots, q_p^B(t) \rangle$ and $\{\Xi_B(t)\} = \langle \mathfrak{I}_1^B(t), \dots, \mathfrak{I}_p^B(t) \rangle^T$ are the vectors of modal responses and generalized forces, respectively. The modal forces $\mathfrak{I}_p^B(t)$ are obtained by projecting the string/body coupling force $F_b(x_b, t)$ (see section 3.3), on the body modal basis. The modal parameters are identified from a single transfer function measurement at the bridge. This fact leads to a requirement that the modal mass matrix should be normalised by postulating all modeshapes $\varphi_p^B(x_b)$ unitary at the bridge location. The physical motions at the bridge are then computed from the modal amplitudes $q_p^B(t)$ and velocities $\dot{q}_p^B(t)$ by superposition:

$$y_b(x_b, t) = \sum_{p=1}^P q_p^B(t); \quad \dot{y}_b(x_b, t) = \sum_{p=1}^P \dot{q}_p^B(t) \quad (13,14)$$

3.3 Formulation of the String/Body Coupling

The coupling between the string and the body of the cello arises from the bridge/string contact force $F_b(x_b, t)$ which is used in equations (2), (10), (11) and (12). In this paper we model this interaction by connecting the string to the bridge through a very stiff spring with some dissipation to avoid any parasitic oscillations of the coupling oscillator:

$$F_b(x_b, t) = K_{bs} \cdot [y_b(x_b, t) - y_s(x_b, t)] + C_{bs} [\dot{y}_b(x_b, t) - \dot{y}_s(x_b, t)] \quad (15)$$

where K_{bs} and C_{bs} are stiffness and damping coupling coefficients between the bridge and the string, and $y_s(x_b, t)$ and $\dot{y}_s(x_b, t)$ are the displacement and velocity of the string at the bridge.

5. SIMULATION RESULTS

We will focus on the movement of a cello C-string with a fundamental frequency of 65.4 Hz, and a linear density of $m = 14 \times 10^{-3}$ kg/m, stopped at the G₃ note, with an effective string length of $L' = 0.3725$ m. In order to achieve adequate computational convergence we have used 80 modes and a sampling frequency of 20000 Hz. A modal damping value of 0.1% was used for all modes (however, frequency dependent damping can be easily introduced with this method) and a string inharmonicity coefficient was introduced to provide more realistic simulations. Concerning the friction model, we chose to use a classic sliding law such as the one presented in equation (7), with $\mu_S = 0.4$, $\mu_D = 0.2$ and $C = 5$, which produced realistic results. For the adherence model a total value of $K_f = 10^5$ N/m as been used. As previously discussed, a near-critical value of the adherence damping term C_f was adopted [3,4]. The body data was obtained from the transfer function measured at the bridge - see [5]. The stiffness and damping constants values, K_{bs} and C_{bs} , used for the string/body coupling were chosen in order to enable a very stiff connection, while keeping a satisfactory computational convergence. We used values of $K_{bs} = 10^8$ N/m and $C_{bs} = 100$ Ns/m. In contrast with previous publications [5], the finger position is kept constant over the G₃ note, where the wolf note should emerge, while the playing conditions, F_N and \dot{y}_{bow} vary exponentially with time.

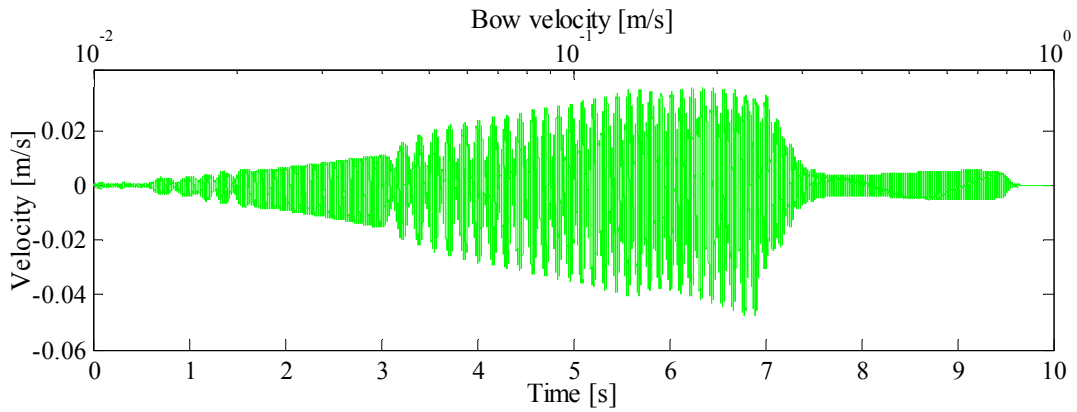


Figure 2 – Simulation of a cello C-string stopped at G_3 with $F_N = 1\text{ N}$ and $\dot{y}_{bow} = 0.01 \sim 1\text{ m/s}$.

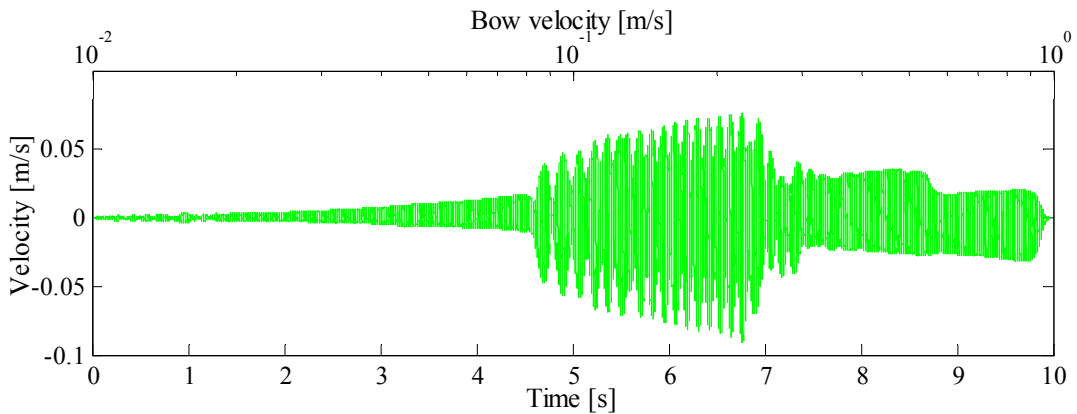


Figure 3 – Simulation of a cello C-string stopped at G_3 with $F_N = 2\text{ N}$ and $\dot{y}_{bow} = 0.01 \sim 1\text{ m/s}$.

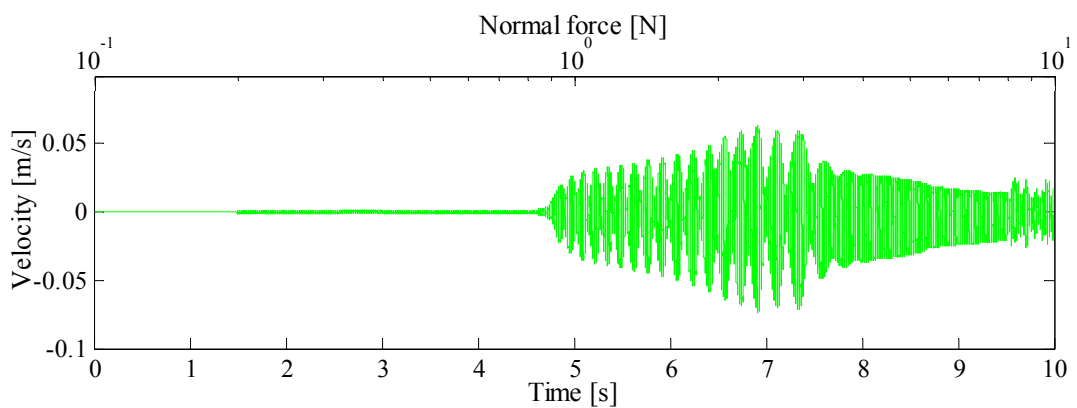
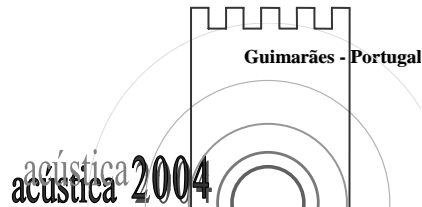


Figure 4 – Simulation of a cello C-string stopped at G_3 with $F_N = 0.1 \sim 10\text{ N}$ and $\dot{y}_{bow} = 0.1\text{ m/s}$.

Figures 2 to 4 represent the bridge velocity time-history for different playing conditions, while the finger position is kept constant. The dependence of the wolf note beating frequency on F_N and \dot{y}_{bow} , can be clearly seen in these figures. As the bow velocity increases so does the wolf note beating frequency, while the opposite behaviour is seen for an increase of the bow normal force.



A fact that is also felt by musicians is the control that can be achieved over the emergence of the wolf note, by applying different bow velocities and normal forces combinations. In the example shown in Figure 2, the wolf note arises when $\dot{y}_{bow} > 0.03$ m/s and disappears when $\dot{y}_{bow} > 0.3$ m/s. If F_N is doubled (Figure 3) the wolf note only emerges when $\dot{y}_{bow} > 0.08$ m/s. Interestingly, if \dot{y}_{bow} is kept constant at 0.1 m/s, the wolf note emerges and disappears at approximately the same time instant, for $F_N > 0.9$ N and $F_N > 3.5$ N, respectively.

5. CONCLUSIONS

In this paper we continue to explore our bowed/plucked string modelling techniques which now incorporate the complex dynamics of real-life instrument bodies, coupled to the string motions. In our hybrid approach, a modelled string interacts with actual or synthesized body data, in the form of bridge impulse response functions or identified modes. Numerical simulations of a cello C-string subjected to varying playing conditions illustrate the interesting behaviour of wolf notes, in particular concerning the dependency of the beating frequency on the bowing parameters.

REFERENCES

- [1] J. Antunes, M. G. Tafasca, L. L. Henrique; *Simulation of the Bowed-String Dynamics: Part 1 – A Nonlinear Modal Approach*, 5e Congrès Français d’Acoustique, Lausanne, Suisse, 3-6 Septembre, 2000.
- [2] M. G. Tafasca, J. Antunes, L. L. Henrique; *Simulation of the Bowed-String Dynamics: Part 2 – Parametric Computations*, 5e Congrès Français d’Acoustique, Lausanne, Suisse, 3-6 Septembre, 2000.
- [3] J. Antunes, L. L. Henrique, O. Inácio; *Aspects of Bowed-String Dynamics*, Proceedings of the 17th International Congress on Acoustics (ICA2001), Rome, Italy, 2001.
- [4] O. Inácio; *Largeur d’Archet et Régimes Dynamiques de la Corde Frottée*, Actes du 6ème Congrès Français d’Acoustique (6ème CFA), Lille, France, 2002.
- [5] O. Inácio, J. Antunes, M.C.M. Wriqth; *On The Violin Family String/Body Dynamical Coupling*, Proceedings of the Institute of Acoustics, Vol. 26, Pt. 2, 2004.
- [6] J. Puaud, R. Caussé & V. Gibiat; *Quasi-périodicité et bifurcations dans la note de loup*, J. Acoustique, Vol. 4, pp. 253-259,1991.
- [7] Firth, J. Buchanan; *The wolf in the cello*, Journal of the Acoustical Society of America, Vol. 53, pp. 457-463,1973.
- [8] H. Benade; *The wolf tone on violin family instruments*, Catgut Acoustical Society Newsletter, Vol. 24, pp. 21-23, 1975.
- [9] M. E. McIntyre, J. Woodhouse; *On the fundamentals of bowed-string dynamics*, Acustica, Vol. 43, pp. 93-108, 1979.
- [10] C. E. Gough; *The resonant response of a violin G-string and the excitation of the wolf note*, Acustica, Vol. 44, pp. 113-123, 1980.
- [11] J. Schelleng; *The Violin as a Circuit*, Journal of the Acoustical Society of America, Vol. 35, pp. 326-338, 1963
- [12] J. Woodhouse; *On the playability of violins: Part 2 – Minimum bow force and transients*, Acustica, Vol. 78, pp. 137-153, 1993.
- [13] J. H. Smith, J. Woodhouse; *The tribology of rosin*, Journal of the Mechanics and Physics of Solids, Vol. 48, pp. 1633-1681, 2000.